RSC Advances

PAPER

View Article Online
View Journal | View Issue

Cite this: *RSC Adv.*, 2025, **15**, 18742

Effect of modified corn stalk combined with ultrasonic conditioning on sludge dewatering performance†

Feng Lin, [a] Siqi Zhang,[a] Jing Ma,*[b] Shuxin Zhang,[a] Baoyu Wang[a] and Huanlei Yang[a]

To address the challenge of high moisture content and difficulty in water removal in sludge, this study optimized the preparation conditions of modified corn stalk powder (MCSP) using solid waste corn stalk powder (CSP) as the raw material. The optimization was achieved through an alkalization–etherification process combined with response surface methodology (RSM). When the optimized MCSP was applied in combination with ultrasonic conditioning for sludge treatment, it was found that the optimal dosage of MCSP was 0.1 g g^{-1} DS. At this dosage, the water content of the dewatered sludge and specific resistance to filtration (SRF) reached their lowest values, which were 1.23 × 10^{12} m kg^{-1} and 53.5%, respectively. Furthermore, the bound water content decreased from 8.53 g g^{-1} DS to 4.64 g g^{-1} DS. There was an increasing trend in the protein and polysaccharide contents across all extracellular polymeric substances (EPS) fractions, with the protein content in soluble EPS (S-EPS) increasing from 4.87 mg g^{-1} to 21.31 mg g^{-1}. At the optimal dosage, the sludge particle size increased to 98.5 μm, and the absolute value of the sludge zeta potential approached zero. The outer boundaries of the flocs became smoother, and the floc structure became more compact, resulting in optimal sludge dewatering performance. Further data analysis revealed that EPS and one-dimensional fractal dimension were the primary factors influencing sludge dewatering performance.

Received 14th February 2025
Accepted 8th May 2025

DOI: 10.1039/d5ra01085c

rsc.li/rsc-advances

1 Introduction

Municipal sludge is a colloidal structural substance composed of bacterial cells, insoluble organics, and other components generated during the water treatment process at urban wastewater treatment plants.[1,2] It contains a substantial amount of heavy metals (such as lead and cadmium), pathogenic bacteria, and other harmful substances (including parasitic ova and aromatic compounds).[3,4] If not properly managed, treated, and disposed of in a manner that is safe, environmentally friendly, and efficient, it can result in significant secondary pollution.[5]

The water content of municipal sludge typically reaches 90% or above, and due to its inherently complex structure, the water contained therein is difficult to remove.[6–8] Generally, free water in sludge can be separated through simple gravitational forces. However, the removal of bound water is significantly more challenging. Extracellular polymeric substances (EPS) accounts for 50% to 90% of the total organic matter in sludge and is the main component of sludge. Moreover, the chemical composition of EPS is highly complex, and its main constituents are similar to those found within microbial cells, including proteins, polysaccharides, humic substances, lipids, nucleic acids, and other organic compounds. These proteins, polysaccharides, and humic substances possess a large number of hydrophilic polar groups (such as hydroxyl, carboxyl, and amino groups) on their surfaces, which can form relatively stable associations with water molecules. This interaction hinders the movement of water between sludge flocs, making dewatering of sludge difficult.[9] Ultimately, this affects subsequent treatment and disposal processes such as incineration and composting.[2,10]

Currently, wastewater treatment plants often employ conditioning agents such as aluminum salts, iron salts, and polyacrylamide (PAM) to treat excess activated sludge. These agents primarily function through compressing the electric double layer, adsorption bridging, and sweep flocculation,[5] destabilizing and aggregating sludge colloids to achieve solid–liquid separation. However, the current method of solely using chemical conditioning combined with mechanical pressure filtration cannot disrupt the EPS structure,[11] cannot ensuring that the water content of sludge below 60%, and fails to meet the requirements for subsequent sludge disposal. Against this backdrop, researchers have attempted to adopt novel dehydration methods, such as electrolysis, photocatalysis, bioflocculants, or bioleaching. Most of these methods aim to improve sludge dewatering performance by disrupting EPS, but

[a]School of Chemical Engineering and Technology, Guangdong Industry Polytechnic University, Guangzhou, China

[b]Automotive Engineering Department, Jining Polytechnic, Jining, China. E-mail: 15603052358@163.com

† Electronic supplementary information (ESI) available. See DOI: https://doi.org/10.1039/d5ra01085c

due to their high investment and operational costs, they are still far from achieving industrialization.

Corn straw (CS) is an important agricultural biomass resource, with an annual production exceeding 200 million tons in China alone. Straw is often regarded as waste and mostly disposed of through stacking or open-air burning, causing severe environmental pollution. Additionally, corn straw is a natural polymer rich in functional groups such as hydroxyl groups, which provide reaction sites for subsequent modifications and increase the likelihood of reactions.[12] Furthermore, corn straw contains a protein colloid called zein, which is easily degradable and can be completely decomposed in soil within 14 days and in water within just 7 days.[13] Therefore, using corn straw as a raw material in sludge dewatering not only poses no adverse effects but, on the contrary, its high calorific value and degradability facilitate subsequent treatment and disposal of the sludge cake.

In this study, agricultural waste corn straw was used as raw material to prepare modified corn straw (MCSP) through alkalization–etherification modification for sludge dewatering. The aim is to reduce the moisture content of sludge under low energy and material consumption conditions, achieving waste treatment by waste utilization. To optimize the conditioning effect, the preparation conditions of MCSP are optimized, and the conditioning process is improved by combining it with ultrasound to further enhance sludge dewatering performance. Through the combination of chemical analysis and data analysis, the changes in the physicochemical properties of sludge are systematically studied, and the key factors influencing deep sludge dewatering performance are thoroughly discussed, further revealing the mechanism of sludge dewatering.

2 Materials and methods

2.1 Experimental materials

The sludge used in this experiment was obtained from a wastewater treatment plant in Guangdong Province, China. The basic properties of the sludge are presented in Text S1 and Table S1 of ESI.†

2.2 Experimental methods

2.2.1 Preparation and optimization of modified corn stalks. Corn straw powder (CSP) was sieved through a 100-mesh sieve and dried before being placed in a beaker. An appropriate amount of NaOH solution was added to alkalinize the CSP at room temperature, followed by the addition of an appropriate amount of cetyltrimethylammonium bromide (CTMAB) solution to conduct an etherification reaction under water bath conditions for several hours. After the alkaline–etherification reaction, the materials in the beaker were washed and filtered with deionized water, repeated three times. The resulting product was then dried in an oven at 105 ± 5 °C to remove free water, subsequently ground, sieved through a 100-mesh sieve for sufficient contact reaction with hydroxyapatite. The final product obtained was the modified corn straw (MCSP), which were placed in a dryer for further use.

2.2.2 Characterization of MCSP. The functional groups of the samples were characterized using Fourier Transform Infrared Spectroscopy (FTIR, VERTEX 70, Bruker, Germany). The binding state variations of the primary elements were analyzed through X-ray Photoelectron Spectroscopy (XPS, K-Alpha, Thermo Scientific, America). The specific surface area and pore size distribution of the samples were determined using a fully automated Brunauer–Emmett–Teller (BET) analyzer (ASAP 2460, Micromeritics, America). Scanning Electron Microscopy (SEM, MIRA LMS, TESCAN, Czech Republic) was employed to analyze the morphological changes of the samples.

2.2.3 Measurement of sludge dewatering performance. The laboratory-scale deep dewatering press is depicted in Fig. S1.† The measurement of water content of the dewatered sludge, specific resistance to filtration (SRF) and bound water content[14] is detailed in ESI (Text S2).†

2.2.4 Analysis of EPS in sludge. An improved thermal extraction method was employed to extract EPS from sludge in Text S3.†[15] The protein content in the extracted EPS fractions was determined using the Coomassie Brilliant Blue method with bovine serum albumin (BSA) as the standard.[16] The polysaccharide content in the extracted EPS fractions was determined using the anthrone method with glucose as the standard.[17]

2.2.5 Particle size and zeta potential analysis. The sludge particle size was measured using a laser diffraction particle size analyzer (MS3000, Malvern). The measurement result was expressed as the median particle size (Dv [50]). The zeta potential of the sludge was measured using a Zeta potential analyzer (Zetasizer Nano-ZS90, Malvern).

2.2.6 Analysis of sludge floc structure. Detailed procedures for the determination of the fractal dimension of floc are described in Text S4.†[18]

2.3 Data analysis

Pearson correlation and factor analysis were conducted using SPSS 17.0 statistical software for data processing.

3 Results and discussion

3.1 Characterization of MCSP

3.1.1 FTIR characterization. To investigate the changes in functional groups between CSP and MCSP, FT-IR analysis was conducted in this study on both samples (Fig. 1). In the MCSP spectrum, the characteristic peak at 3425.9 cm^{-1} and the CSP spectrum at 3418 cm^{-1} represent hydroxyl groups. Additionally, the absorption peaks at 2919, 1730, 1514, 1248, and 1053 cm^{-1} in the CSP spectrum correspond to the stretching vibrations of –C–H, –C=O, C=C, –C–O, and –C–O–C, respectively. These peaks primarily originate from glucose and polysaccharides present in the raw cellulose and starch.[19,20] After the alkalization–etherification reaction, the absorption peaks at 1514 and 1248 cm^{-1} disappeared, indicating the opening of oxygen-containing heterocycles due to modification.[21] In the MCSP spectrum, the peaks at 2928.3, 2858.9, and 899.6 cm^{-1} represent

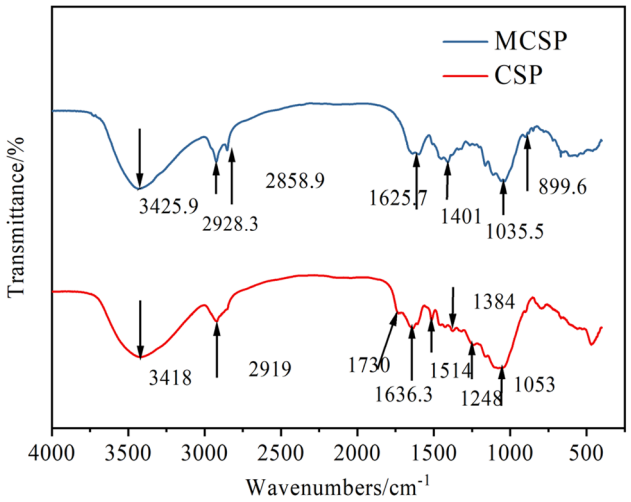

Fig. 1 Infrared spectrogram.

N–CH_3, –CH_2–N–CH_2–, and C–Br absorption peaks, respectively, demonstrating the successful loading of the quaternary ammonium groups from CTMAB onto the surface of CSP through etherification reaction.[22] The modification imparts positive charges to MCSP, enabling it to undergo electrostatic neutralization when added to sludge systems. This facilitates the adsorption and aggregation of colloidal particles within the sludge, thereby enhancing sludge dewatering performance. The FTIR analysis of CSP and MCSP in the 1500–1800 cm^{-1} region was shown in Text S5.†

3.1.2 Characterization of surface topography. As shown in Fig. 2, CSP exhibits a fibrous structure, which is attributed to the cellulose and lignin content accounting for approximately 60% of the total components.[23] As shown in Fig. 2c and d, pores appeared in the sample after the alkali etheration reaction. The increase in the specific surface area of MCSP from 1.23 m^2 g^{-1} to 1.35 m^2 g^{-1} in Table 1 indicates that there are more active sites on the surface of MCSP. This further demonstrates that the adsorption capacity of MCSP has been significantly enhanced, enabling it to adsorb more pollutants. The average pore size increasing from 19.65 nm to 22.76 nm suggests that the pore structure of MCSP has become more spacious. Larger pores facilitate the adsorption of larger-sized pollutants, thereby improving adsorption efficiency. The increase in pore volume also means that there is more space within MCSP to accommodate adsorbed substances, further increasing the adsorption capacity. MCSP presents a flake-like morphology, with flakes evenly distributed on the inner side of the pores and the surface of the sample. This indicates that the structure of the original material becomes looser and more accessible after the alkali–etherification reaction. Compared to CSP, the formation of pores in the MCSP sample facilitates the penetration of moisture into the polymer, thereby improving its solubility.[24] Additionally, the multilayer three-dimensional network structure of MCSP provides a large number of contact points, enabling the

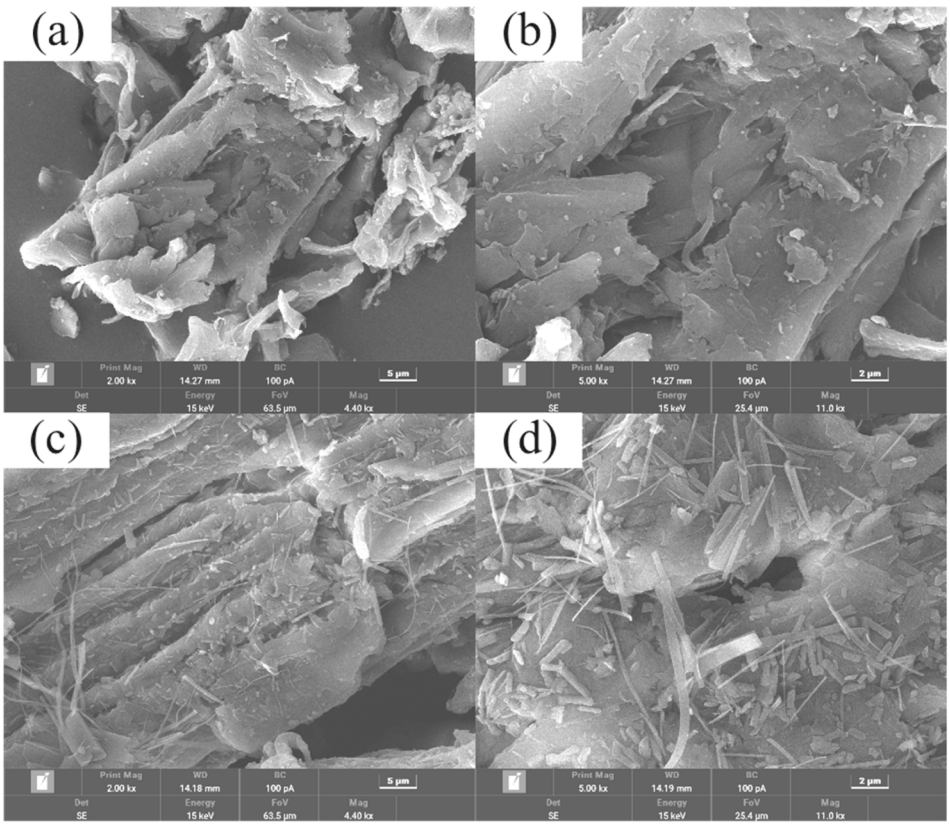

Fig. 2 SEM image analysis (a) and (b) CSP; (c) and (d) MCSP.

Table 1 Specific surface area parameter

Sample	BET surface area	Adsorption average pore diameter	BJH adsorption cumulative volume of pores
CSP	1.23 $m^2 g^{-1}$	19.65 nm	0.0048 $cm^3 g^{-1}$
MCSP	1.35 $m^2 g^{-1}$	22.76 nm	0.0051 $cm^3 g^{-1}$

adsorbent to interact with colloidal particles through van der Waals forces, thereby accommodating and immobilizing the adsorbed colloidal particles. Moreover, the quaternary ammonium groups introduced through etherification impart a positive charge to the surface of MCSP. These positive charges can neutralize the negative charges on the surface of sludge particles, reducing the electrostatic repulsion between particles. This facilitates the adsorption process and promotes particle aggregation and flocculation. Ultimately, this contributes to enhanced sludge dewatering performance.

3.1.3 XPS. XPS spectroscopic analysis was conducted on CSP and MCSP to investigate the similarities and differences in the elemental species present on the surface of the samples before and after modification, with the characterization results presented in Fig. S2.† Both CSP and MCSP are predominantly composed of C, N, and O. Notably, compared to the full spectrum of CSP, the emergence of Na 1s and Br 3d absorption peaks in MCSP indicates that the alkalization–etherification process successfully loaded Na and Br elements onto CSP. A comparison between Fig. S2(a) and (d)† reveals that C–C bonds dominate in both CSP and MCSP, with the MCSP spectrum additionally containing C–N^+ and O=C–N bonds,[25] confirming the immobilization of quaternary ammonium groups onto the CSP surface. Following the modification of CSP, a decrease in the proportion of C–N bonds and the emergence of C–N^+ bonds suggest the quaternization of CSP (Fig. S2 (c) and (f)†). Simultaneously, the binding energy positions at 531.0 eV and 531.80 eV in both CSP and MCSP correspond to –OH and C–O bonds, respectively, primarily associated with groups in alcohols, hemiacetals, or acetals, which are typically closely related to polysaccharides in CSP and MCSP.[26,27] The binding energy positions at 533.36 eV and 532.64 eV correspond to O–C=O and C=O bonds, respectively, primarily associated with groups in carbonyls, carboxylates, and amide esters, indicating that MCSP retains its original structure after modification.

3.2 Effect of MCSP on sludge dewatering performance

Through single-factor experiments, the effects of factors during the preparation of MCSP on sludge dewatering performance were investigated. Based on the optimal value ranges of factors A (alkali concentration), B (alkalization time), C (etherification temperature), and E (etherification concentration) determined through single-factor experiments, the water content of the dewatered sludge was selected as the response variable (R1). The Box–Behnken design of response surface method (RSM) was used to optimize the preparation conditions of MCSP. For detailed analysis, see ESI Text S6, Table S2 and Fig. S3 and S4.†

3.2.1 Effect of MCSP conditioning alone on sludge dewatering performance. Fig. 3 depicts the variation in sludge dewatering performance under different dosages of MCSP conditioning. With the increase in MCSP dosage, both the water content and SRF of the sludge exhibit a trend of initial decrease followed by an increase. Optimal dewatering effect is achieved when the MCSP dosage is 0.15 g g^{-1} DS, resulting in a reduced water content to 61.56% and a decreased SRF to 5.13 × 10^{12} m kg^{-1}. This is attributed to the negatively charged nature of the sludge system, whereas the dewatering agent MCSP carries positive charges. These positive charges neutralize the negative charges present in the sludge, thereby weakening the electrostatic repulsion between sludge particles. However, an excessive amount of MCSP leads to an excess of positive charges in the sludge system, causing the particles to once again repel electrostatically and become difficult to aggregate.[28] This hinders the release of bound water within the system, ultimately impeding the filtration and dewatering of the sludge.

3.2.2 Effect of MCSP combined with ultrasonic conditioning on sludge dewatering performance. From Fig. 4, both the water content and SRF of the sludge exhibit a trend of initial decrease followed by an increase as the MCSP dosage increases. At an MCSP dosage of 0.1 g g^{-1} DS, the water content of the dewatered sludge and SRF reach their lowest values, which are 1.23 × 10^{12} m kg^{-1} and 53.5%, respectively, showing a significant reduction compared to sludge samples without ultrasonic assistance. Fig. 4b reveals the impact of the combination of MCSP and ultrasonication on bound water content, which decreases from 8.53 g g^{-1} DS to 4.64 g g^{-1} DS. This may be attributed to the synergistic effect of ultrasonication and MCSP conditioning. On the one hand, ultrasonication generates

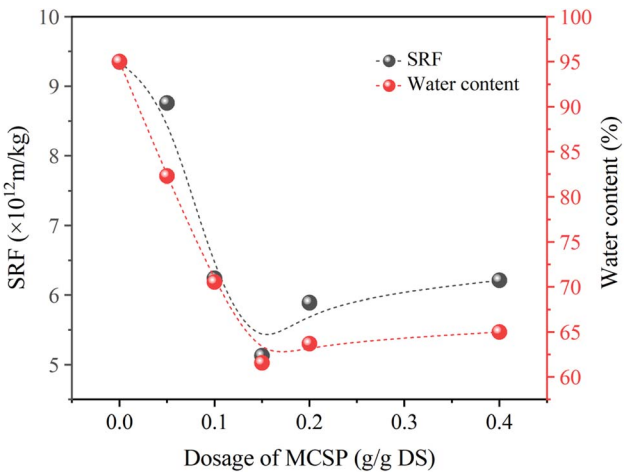

Fig. 3 Effect of MCSP dosage on sludge dewatering performance.

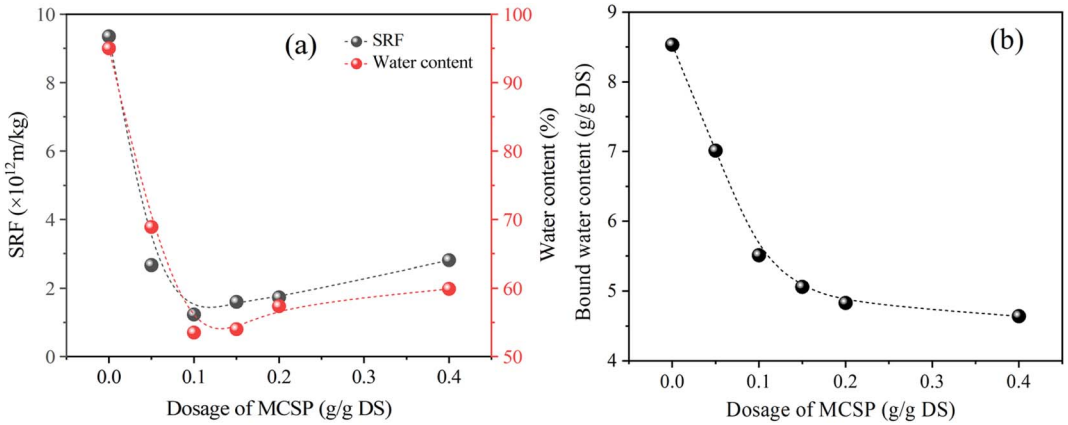

Fig. 4 Impact of combined conditioning on sludge dewatering performance (a) SRF and water content; (b) bound water content.

sonochemical effects, including instantaneous high temperature and pressure as well as shear forces, which can disrupt cellular structures and decompose refractory organics. On the other hand, it creates a sponge effect, allowing water to more easily pass through channels produced by wave propagation, thereby promoting the increase in sludge aggregation particle size.[29] This conversion of surface-bound water into free water alters the water distribution in the sludge, leading to significant improvements in both SRF and the water content of the dewatered sludge.

3.3 Impact of combined conditioning with MCSP and ultrasonication on sludge properties

3.3.1 EPS. The composition and spatial distribution of EPS are closely related to the bioflocculation, settlement, and dewatering performance of sludge, with protein (PN) and polysaccharide (PS) typically recognized as the primary components of EPS, accounting for 75–89% of the total organic carbon (TOC) in sludge.[30] As shown in Fig. 5, after combined conditioning with MCSP and ultrasonication, the protein content in EPS fractions exhibited an increasing trend. Specifically, the protein content in S-EPS increased from 4.87 mg g^{-1} to 21.31 mg g^{-1}, in LB-EPS from 2.12 mg g^{-1} to 12.7 mg g^{-1}, and in TB-EPS from 1.65 mg g^{-1} to 16 mg g^{-1}. Similarly, the polysaccharide content in EPS also demonstrated an increasing trend. Notably, the protein and polysaccharide contents in S-EPS were higher than those in LB-EPS and TB-EPS. This may be attributed to the quaternary ammonium groups loaded onto the MCSP structure disrupting sludge cells, reducing the activity of planktonic cells within the sludge, disturbing the stable sludge system, and altering intracellular and extracellular osmotic pressures. Consequently, intracellular bound water and encapsulated organics are released into the system. Additionally, the positive charges carried by MCSP neutralize the negative charges present in the sludge system, disrupting the EPS structure and releasing encapsulated proteins, polysaccharides, and other organics into the filtrate. On the other hand, the introduction of ultrasonication disrupts the cell wall structure, releasing intracellular materials and causing some loosely and tightly bound EPS components to dissolve and transfer to S-EPS and the supernatant. Therefore, under the combined action of MCSP

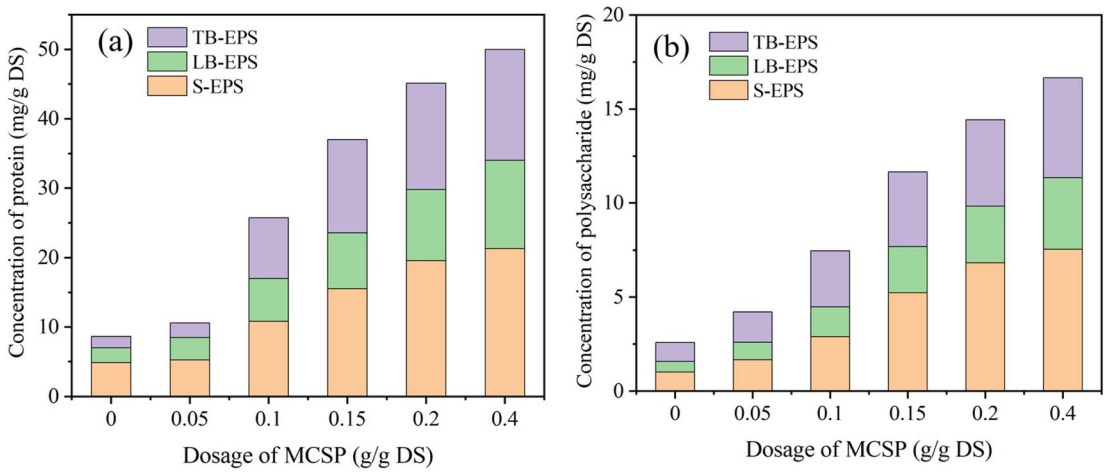

Fig. 5 Impact of combined conditioning with MCSP and ultrasonication on EPS (a) protein and (b) polysaccharide.

and ultrasonication, the content of protein and polysaccharide in S-EPS is relatively high.

3.3.2 Particle size, zeta potential, and fractal dimension. As illustrated in Fig. 6, under the assistance of ultrasonic treatment, the sludge particle size exhibits a trend of initially increasing and then decreasing with the increasing dosage of MCSP. Specifically, when the MCSP dosage reaches 0.1 g g^{-1} DS, the sludge particle size increases from 43.5 μm to 98.5 μm, achieving a maximum value. Simultaneously, as the MCSP dosage gradually increases, the zeta potential of the sludge samples shifts from negative to positive. At a dosage of 0.1 g g^{-1} DS, the absolute value of the zeta potential of the sludge approaches zero, indicating that the negative charges in the sludge system are gradually neutralized by the positive charges carried by MCSP. This leads to the rapid aggregation of unstable colloidal particles in the system, resulting in the maximum sludge particle size and optimal sludge dehydration performance. However, as the MCSP dosage continues to increase, the absolute value of the zeta potential of the sludge increases, and an excessive amount of positive charges in the system forms a stable system with opposite charges once again, which is unfavorable for the occurrence of re-aggregation reactions. Consequently, the sludge particle size decreases. The presence of fine particles in the sludge system can block the pore structure formed during the filtration process, making it difficult for the bound water in the sludge system to be released and drained.[31] Therefore, the sludge SRF and water content increase, deteriorating the dewatering performance.

D1 represents the irregularity or roughness of the boundary of floc particles. A value closer to 1 indicates a less irregular and smoother boundary surface of the floc. D2 indicates the compactness of the floc, with a higher D2 value suggesting a more dense floc structure.[22] A higher D1 value is typically associated with lower dewatering performance, as a rougher surface increases the friction between particles, hindering the expulsion of water. Conversely, a higher D2 value is usually linked to better dewatering performance, since a more compact structure helps to reduce the pores between particles, enhancing the strength and stability of the flocs, thereby improving dewatering performance. As shown in Fig. 6, the raw sludge has a D1 value of 1.23 and a D2 value of 1.12. After combined conditioning with MCSP and ultrasound, D1 gradually decreases while D2 continuously increases. This indicates that during the flocculation process, the outer boundary of the floc becomes smoother and the floc structure becomes more dense. This is due to the combined effect of MCSP and ultrasound, which allows the released intracellular organic matter to enter the EPS and encapsulates the previously exposed inorganic particles, thereby smoothing their boundaries. The continuous increase in D2 is closely related to the decrease in the absolute value of the sludge zeta potential. As the electrostatic repulsion between sludge particles decreases, the force compressing the electric double layer increases, resulting in the formation of more dense flocs.

3.4 Analysis of key factors influencing the sludge dewaterability

3.4.1 Pearson correlation analysis. To investigate the sludge dewatering mechanism, this section examines the correlation between sludge dewatering performance and selected physicochemical properties of sludge, including EPS,

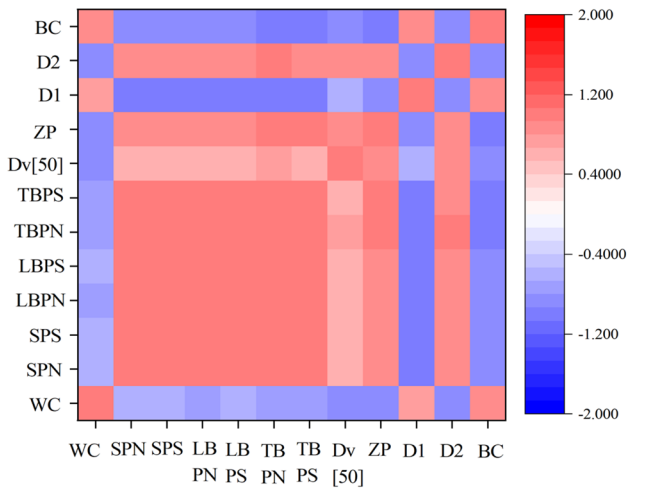

Fig. 7 Pearson correlation analysis.

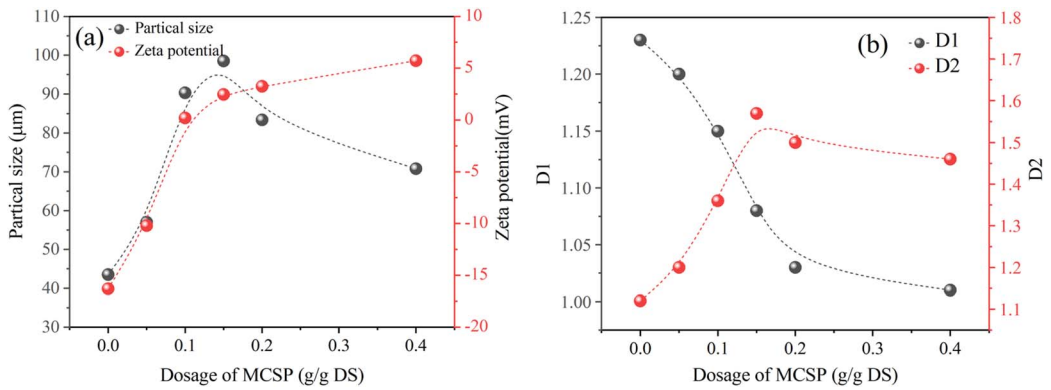

Fig. 6 Effects of MCSP combined with ultrasonic conditioning on sludge particle size, zeta potential, and fractal dimension (a) particle size and zeta potential; (b) fractal dimension.

particle size, zeta potential, fractal dimension, and bound water content. Fig. 7 and Table S3† present the Pearson correlation coefficients between sludge dewatering performance and these physicochemical properties. The correlation coefficients between EPS, particle size, zeta potential, fractal dimension, bound water content, and the water content of the dewatered sludge are all greater than 0.6, indicating a strong correlation between these sludge physicochemical properties and dewatering performance.[32,33] Among them, D1 and bound water content exhibit a positive correlation with water content of the dewatered sludge, while protein and polysaccharide in EPS, particle size, zeta potential, and D2 show a negative correlation. Notably, particle size, zeta potential, D2, and bound water content demonstrate an extremely strong correlation with the water content of the dewatered sludge.

3.4.2 Factor analysis. Based on the above analysis, it is evident that particle size, zeta potential, and EPS all significantly influence sludge dewatering performance. However, multicollinearity exists among most of these indicators. Therefore, factor analysis, a multivariate statistical method, was employed to simplify multiple independent indicators into a few comprehensive indicators while minimizing the loss of original information and reducing the number of variables as much as possible.[34] This method aims to capture as much information from the original variables as possible using a limited number of variables. Factor analysis was conducted on 11 standardized variables (particle size, zeta potential, protein and polysaccharide in three-layer EPS, D1, D2, and bound water), and the results are presented in Table S4.† It can be observed that the cumulative variance contribution rate of the first three common factors is 99.68%, encompassing most of the information from the 11 variables. This is also evident from the scree plot (Fig. S5†). Therefore, three common factors were selected for this study. Additionally, through orthogonal rotation, the gap between the characteristic root values narrowed, with the initial maximum characteristic root value being 10.023 and the minimum being 0.11, which changed to a maximum of 7.283 and a minimum of 0.128 after rotation. This indicates that the rotation reduced the variance contribution rate disparity among the factors, resulting in a more balanced overall explanatory power.

Table S5† presents the factor loading matrix, where the loadings of the 11 variables on the first factor are high both before and after rotation, indicating a strong correlation with the first factor. After applying orthogonal rotation to the factor loading matrix using the varimax method, the cumulative contribution rate of factor 1 reached 91.118%, while the contribution rates of factors 2 and 3 were only 7.564% and 0.998%, respectively. Therefore, factor 1 is the most significant influencing factor. Among them, EPS and D1 have relatively high loadings on factor 1 both before and after rotation, indicating that they are the primary factors affecting sludge dewatering performance.

The chemical composition and structure of EPS significantly influence the sludge dewatering performance. Disrupting the network structure of EPS can release bound water, reduce the water-holding capacity of sludge, and thereby enhance dewatering performance. The degradation of EPS also makes the sludge floc structure more porous, with the released organic matter encapsulating previously exposed inorganic particles and smoothing the floc boundaries, leading to a decrease in D1. A lower D1 value typically indicates better dewatering performance, as smoother surfaces reduce inter-particle friction and facilitate water expulsion. Therefore, the composition and structure of EPS, as well as D1, are key factors affecting sludge dewatering performance. Optimizing the degradation of EPS and the regulation of floc structure can significantly improve sludge dewatering performance, providing a theoretical basis for the development of more efficient sludge treatment and disposal methods.

3.4.3 Mechanism analysis. As shown in Fig. S6† and 8, MCSP has been subjected to alkali–etherification treatment, introducing cationic groups (such as quaternary ammonium groups) that impart a positive charge to its surface. EPS, primarily composed of proteins, polysaccharides, and nucleic acids, typically carries a negative charge. As a result, there is a significant electrostatic interaction between MCSP and EPS. This interaction can neutralize the negative charges within EPS, disrupting its original structural stability. The electrostatic neutralization not only alters the charge distribution of EPS but may also affect the conformation of proteins and polysaccharides within EPS, causing them to shift from a compact structure to a more relaxed state. This structural change can lead to the release of bound water within EPS, thereby reducing its bound water content.

Ultrasonication, through the cavitation effect generated by high-frequency vibrations, can disrupt the structure of sludge cell walls and EPS.[35] This physical fragmentation can release intracellular bound water and organic matter, further reducing

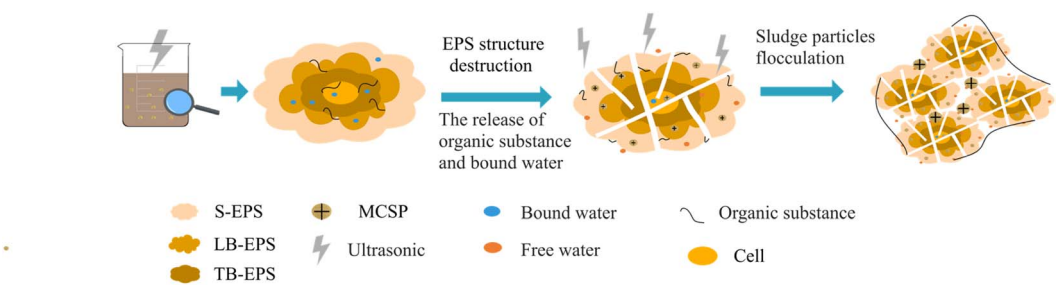

Fig. 8 Sludge dewatering mechanism.

the bound water content within EPS. Additionally, the shear forces from ultrasonication can break down the EPS network structure, allowing the substances encapsulated within EPS to be further released and dissolved.[35,36] However, the small sludge flocs that have been disrupted may reaggregate due to the addition of the dewatering agent MCSP, re-flocculation after ultrasonication, and the sweeping and adsorption effects of the released EPS on them. These tiny particles reaggregate into larger floc structures, facilitating the removal of water by external forces in subsequent steps. Therefore, ultrasonication-assisted MCSP conditioning can produce a synergistic effect that further improves the dewatering performance of sludge.

4 Conclusion

In this study, waste corn stalks were used to prepare MCSP through an alkalization–etherification process to enhance sludge dewatering performance. Characterization confirmed the successful modification of MCSP. When combined with ultrasound for sludge conditioning, the optimal MCSP dosage was 0.1 g g^{-1} DS. At this dosage, the water content and SRF reached their lowest values of 53.5% and 1.23×10^{12} m kg^{-1}, respectively, significantly lower than those of sludge samples without ultrasound-assisted conditioning. The bound water content decreased from 8.53 g g^{-1} DS to 4.64 g g^{-1} DS, and the protein and polysaccharide contents in S-EPS were higher than those in LB-EPS and TB-EPS. The sludge particle size initially increased to 98.5 μm from 43.5 μm at an MCSP dosage of 0.1 g g^{-1} DS. The absolute value of the zeta potential approached zero, reducing electrostatic repulsion between sludge particles and leading to denser flocs with increasing D2. Combining data analysis with mechanistic insights revealed that EPS and D1 were the primary factors influencing sludge dewatering performance.

Data availability

The data supporting this article have been included as part of the ESI.†

Author contributions

All authors made contributions to the study conception and design. Material preparation, data collection and analysis were carried out by Feng Lin and Jing Ma. The first draft of the manuscript was completed by Feng Lin and Shuxin Zhang commented on previous versions of the manuscript. The final manuscript was read and approved by Baoyu Wang, Huanlei Yang and Siqi Zhang.

Conflicts of interest

The authors declare that they have no competing interests.

Acknowledgements

The current study was supported by the Project of Educational Commission of Guangdong Province of China (2022KQNCX172 and 2023KTSCX248), Science and Technology Program of Guangzhou, China (2023A04J1635 and 202201011363), University's Educational and Teaching Reform Project on "Ideological and Political Education in Courses" (KCSZ202415), and Exquisite Education Project of Guangdong Industry Polytechnic University (JZYR202416).

References

1 H. Xia, J. Tang, L. Aljerf, C. Cui, B. Gao and P. O. Ukaogo, Dioxin emission modeling using feature selection and simplified dfr with residual error fitting for the grate-based mswi process, *Waste Manage.*, 2023, **168**, 256–271, DOI: 10.1016/j.wasman.2023.05.056.

2 T. Wang, J. Tang, L. Aljerf, J. Qiao and M. Alajlani, Emission reduction optimization of multiple flue gas pollutants in municipal solid waste incineration power plant, *Fuel*, 2025, **381**(PartA), 133382, DOI: 10.1016/j.fuel.2024.133382.

3 H. Xia, J. Tang, L. Aljerf, T. Wang, B. Gao, Q. Xu, Q. Wang and P. O. Ukaogo, Assessment of PCDD/Fs formation and emission characteristics at a municipal solid waste incinerator for one year, *Sci. Total Environ.*, 2023, **883**, 163705, DOI: 10.1016/j.scitotenv.2023.163705.

4 H. Xia, J. Tang, L. Aljerf, T. Wang, B. Gao and M. Alajlani, AI-based tree modeling for multi-point dioxin concentrations in municipal solid waste incineration, *J. Hazard. Mater.*, 2024, **480**, 135834, DOI: 10.1016/j.jhazmat.2024.135834.

5 P. Yang, D. Li, W. Zhang, N. Wang, Z. Yang, D. Wang and T. Ma, Flocculation-dewatering behavior of waste activated sludge particles under chemical conditioning with inorganic polymer flocculant: Effects of typical sludge properties, *Chemosphere*, 2019, **218**, 930–940, DOI: 10.1016/j.chemosphere.2018.11.169.

6 H. Masihi and G. B. Gholikandi, Employing Electrochemical-Fenton process for conditioning and dewatering of anaerobically digested sludge: A novel approach, *Water Res.*, 2018, **144**, 373–382, DOI: 10.1016/j.watres.2018.07.054.

7 P. Bao, C. Du, Y. Li, H. Jiang, L. Zhou, G. Yu, S. Sun, L. Zhou, X. Li and J. Teng, Application of skeleton builders to sludge dewatering and disposal: a critical review, *Sci. Total Environ.*, 2024, **906**, 167106, DOI: 10.1016/j.scitotenv.2023.167106.

8 S. He, L. Zhao, Y. Liu, L. Feng, T. Hu, Z. Gao, L. Wei and S. You, Multiple drivers and mechanisms of solid-water interfacial interactions in sludge dewatering: Roles of polarity and molecular structure of extracellular polymeric substances, *Water Res.*, 2024, **263**, 122180, DOI: 10.1016/j.watres.2024.122180.

9 D. Zhang, Y. Wang, H. Gao, X. Fan, Y. Guo, H. Wang and H. Zheng, Variations in macro and micro physicochemical properties of activated sludge under a moderate oxidation-in situ coagulation conditioning: relationship between molecular structure and dewaterability, *Water Res.*, 2019, **155**, 245–254, DOI: 10.1016/j.watres.2019.02.047.

10 Y. Q. Liang, J. Tang, H. Xia, L. Aljerf, B. Y. Gao and M. L. Akel, Three-dimensional numerical modeling and analysis for the municipal solid-waste incineration of the grate furnace for particulate-matter generation, *Sustainability*, 2023, **15**, 12337, DOI: 10.3390/su151612337.

11 H. F. Wang, H. J. Wang, H. Hu and R. J. Zeng, Applying rheological analysis to understand the mechanism of polyacrylamide (PAM) conditioning for sewage sludge dewatering, *RSC Adv.*, 2017, **7**, 30274–30282, DOI: 10.1039/C7RA05202B.

12 S. Guo, J. Tan, D. Zhao, Z. Liu, C. Zhao, X. Li and G. Li, Co-hydrothermal carbonization of sewage sludge and corn straw: Physicochemical properties and gasification performance *via* process simulation using Aspen plus, *J. Environ. Chem. Eng.*, 2023, **11**, 110794, DOI: 10.1016/j.jece.2023.110794.

13 E. Corradini, P. S. Curti, A. B. Meniqueti, A. F. Martins, A. F. Rubira and E. C. Muniz, Recent advances in food-packing, pharmaceutical and biomedical applications of zein and zein-based materials, *Int. J. Mol. Sci.*, 2014, **15**, 22438–22470, DOI: 10.3390/ijms151222438.

14 J. Liu, Y. Wei, K. Li, J. Tong, Y. Wang and R. Jia, Microwave-acid pretreatment: a potential process for enhancing sludge dewaterability, *Water Res.*, 2016, **90**, 225–234, DOI: 10.1016/j.watres.2015.12.012.

15 X. Y. Li and S. F. Yang, Influence of loosely bound extracellular polymeric substances (EPS) on the flocculation, sedimentation and dewaterability of activated sludge, *Water Res.*, 2007, **41**, 1022–1030, DOI: 10.1016/j.watres.2006.06.037.

16 M. M. Bradford, A rapid and sensitive method for the quantitation of microgram quantities of protein utilizing the principle of protein-dye binding, *Anal. Biochem.*, 1976, **72**, 248–254, DOI: 10.1016/0003-2697(76)90527-3.

17 K. Raunkjær, J. T. Hvitved and P. H. Nielsen, Measurement of pools of protein, carbohydrate and lipid in domestic wastewater, *Water Res.*, 1994, **28**, 251–262, DOI: 10.1016/0043-1354(94)90261-5.

18 P. Zhao, S. Ge, Z. Chen and X. Li, Study on pore characteristics of flocs and sludge dewaterability based on fractal methods (pore characteristics of flocs and sludge dewatering), *Appl. Therm. Eng.*, 2013, **58**, 217–223, DOI: 10.1016/j.applthermaleng.2013.03.01.

19 J. Baeza and J. Freer, Chemical characterization of wood and its components, *Wood Cellul. Chem.*, 2000, **2**, 275–384.

20 Q. Lin, H. Peng, S. Zhong and J. Xiang, Synthesis, characterization, and secondary sludge dewatering performance of a novel combined silicon–aluminum–iron–starch flocculant, *J. Hazard. Mater.*, 2015, **285**, 199–206, DOI: 10.1016/j.jhazmat.2014.12.005.

21 Z. Zhang, H. Zheng, F. Huang, X. Li, S. He and C. Zhao, Template polymerization of a novel cationic polyacrylamide: sequence distribution, characterization, and flocculation performance, *Ind. Eng. Chem. Res.*, 2016, **55**, 9819–9828, DOI: 10.1021/acs.iecr.6b01894.

22 X. Zhao, J. Chen, F. Chen, X. Wang, Q. Zhu and Q. Ao, Surface characterization of corn stalk superfine powder studied by FTIR and XRD, *Colloids Surf., B*, 2013, **104**, 207–212, DOI: 10.1016/j.colsurfb.2012.12.003.

23 Y. Zeng, Z. Liu, E. Hu, J. Yu, Q. Xiong, Y. Tian and S. Li, Insight into impact of co-pyrolysis process parameters on cross-interaction of volatiles between furfural residue and coal *via* rapid infrared heating, *Energy*, 2024, **309**, 133118, DOI: 10.1016/j.energy.2024.133118.

24 F. Guo, C. Wang, S. Wang, S. Wu, X. Zhao and G. Li, Fenton-ultrasound treatment of corn stalks enhances humification during composting by stimulating the inheritance and synthesis of polyphenolic compounds—preliminary evidence from a laboratory trial, *Chemosphere*, 2024, **358**, 142133, DOI: 10.1016/j.chemosphere.2024.142133.

25 S. Karamdoust, B. Yu and C. V. Bonduelle, Preparation of antibacterial surfaces by hyperthermal hydrogen induced cross-linking of polymer thin films, *J. Mater. Chem.*, 2012, **22**, 4881–4889, DOI: 10.1039/C2JM15814K.

26 L. Zhou, W. Q. Zhuang and Y. G. De Costa, In situ and short-time anaerobic digestion coupled with alkalization and mechanical stirring to enhance sludge disintegration for phosphate recovery, *Chem. Eng. J.*, 2018, **351**, 878–885, DOI: 10.1016/j.cej.2018.06.156.

27 C. S. Lee, M. F. Chong, J. Robinson and E. Binner, Optimisation of extraction and sludge dewatering efficiencies of bio-flocculants extracted from Abelmoschus esculentus (okra), *J. Environ. Manage.*, 2015, **157**, 320–325, DOI: 10.1016/j.jenvman.2015.04.028.

28 J. Hou, Y. Hu, Z. Yang, J. Wu, G. You, Y. Fan and L. Miao, Synergistic coupling of flocculation and fenton reaction for enhanced sludge dewatering: Pivotal role of bi-functional cationic tannin, *Chem. Eng. J.*, 2024, **491**, 152058, DOI: 10.1016/j.cej.2024.152058.

29 H. M. Ruiz, E. Cabanillas, J. Labanda and J. Llorens, Ultrasound, thermal and alkali treatments affect extracellular polymeric substances (EPSs) and improve waste activated sludge dewatering, *Process Biochem.*, 2015, **50**, 438–446, DOI: 10.1016/j.procbio.2015.01.001.

30 W. Zhang, P. Yang, X. Yang, Z. Chen and D. Wang, Insights into the respective role of acidification and oxidation for enhancing anaerobic digested sludge dewatering performance with Fenton process, *Bioresour. Technol.*, 2015, **181**, 247–253, DOI: 10.1016/j.biortech.2015.01.003.

31 C. Chen, T. Zhang, L. Lv, Y. Chen, W. Tang and S. Tang, Destroying the structure of extracellular polymeric substance to improve the dewatering performance of waste activated sludge by ionic liquid, *Water Res.*, 2021, **199**, 117161, DOI: 10.1016/j.watres.2021.117161.

32 Q. Dai, L. Ma, N. Ren, P. Ning, Z. Guo, L. Xie and H. Gao, Investigation on extracellular polymeric substances, sludge flocs morphology, bound water release and dewatering performance of sewage sludge under pretreatment with modified phosphogypsum, *Water Res.*, 2018, **142**, 337–346, DOI: 10.1016/j.watres.2018.06.009.

33 B. Wu, H. Wang, X. Dai and X. Chai, Influential mechanism of water occurrence states of waste-activated sludge: specifically focusing on the roles of EPS micro-spatial

distribution and cation-dominated interfacial properties, *Water Res.*, 2021, **202**, 117461, DOI: **10.1016/j.watres.2021.117461**.

34 Y. Wei, L. U. Wen, L. Ping and P. Y. Zhong, Application of factor analysis method to the water quality evaluation of Yitong River, *Research of Soil and Water Conservation*, 2007, **14**, 113–114.

35 G. J. Xie, B. F. Liu, Q. Wang, J. Ding and N. Q. Ren, Ultrasonic waste activated sludge disintegration for recovering multiple nutrients for biofuel production, *Water Res.*, 2016, **93**, 56–64, DOI: **10.1016/j.watres.2016.02.012**.

36 H. Jia, B. Liu, X. Zhang, J. Chen and W. Ren, Effects of ultrasonic treatment on the pyrolysis characteristics and kinetics of waste activated sludge, *Environ. Res.*, 2020, **183**, 109250, DOI: **10.1016/j.envres.2020.109250**.